Flexible organic photovoltaics from zinc oxide nanowires grown on transparent and conducting single walled carbon nanotube thin films

Husnu Emrah Unalan,*[a] Pritesh Hiralal,[a] Daniel Kuo,[a] Bhavin Parekh,[b] Gehan Amaratunga[a] and Manish Chhowalla[b]

The fabrication of flexible organic photovoltaics (OPVs) which utilize transparent and conducting single walled carbon nanotube (SWNT) thin films as current collecting electrodes on plastic substrates in zinc oxide nanowire (ZnO NW)/poly(3-hexylthiophene) (P3HT) bulk heterojunction photovoltaic devices is reported. The bulk heterojunctions for exciton dissociation are created by directly growing ZnO nanowires from solution on the SWNT electrodes and spin coating the P3HT polymer. A maximum OPV power conversion efficiency of ~0.6% was achieved. Our results indicate that nanotube–nanowire hybrids fabricated *via* solution based methods are promising for optoelectronic and energy harvesting devices.

Introduction

Organic photovoltaics (OPVs) based on semiconducting polymers offer low cost, light weight and flexible alternatives to their inorganic counterparts.[1,2] OPVs can be fabricated using simple solution based deposition techniques that are compatible with roll-to-roll processing. Current state-of-the-art OPVs are based on a mixture of conjugated polymer as electron donors and fullerene as electron acceptors.[3–7] Power conversion efficiencies of ~5% have been reported for the bulk heterojunction P3HT/phenyl-C61-butyric acid methyl ester (PCBM) solar cells.[8,9]

Current research in bulk heterojunction OPVs is geared towards: *i*) exploration of novel materials with low bandgap,[10,11] *ii*) device optimization through polymer morphology control,[12,13] and *iii*) stability studies.[14,15] Most photovoltaic devices utilize an indium tin oxide (ITO) coated substrate as a transparent and conducting electrode. ITO requires vacuum deposition and is expensive due to the limited supply of indium. ITO also cracks when flexed due to its crystalline nature, making it incompatible with flexible OPVs. Attempts to replace ITO include using silver grids in conjunction with highly conducting poly(3,4-ethylenedioxythiophene)/poly(styrenesulfonate) PEDOT:PSS,[16] vapor phase polymerized PEDOT,[17] silver nanowire[18] and single walled carbon nanotube (SWNT) thin films.

Carbon nanotubes have already been utilized in OPVs by a number of researchers. Kymakis *et al.* used SWNTs as electron acceptors in a poly(3-octyl)thiophene matrix,[19] whereas Ago *et al.*[20] and Miller *et al.*[21] used pristine and functionalized MWNTs as hole collecting electrodes in OPVs, respectively. In our previous work, we showed that SWNT thin films deposited from solution can be used to replace ITO in OPVs.[22] It has also been demonstrated that SWNT thin films can be used to fabricate flexible OPVs, making them a step closer to roll-to-roll processing.[23] Although the sheet resistance of SWNT thin films is still higher than that of ITO, the three dimensional skeletal nature of the interface between SWNTs and the organic layer makes them efficient hole collectors in OPVs.[22]

Despite the promising results obtained with P3HT/PCBM bulk heterojunction devices, the disordered structure of the nanocomposite limits the performance of the OPVs. Power conversion efficiencies are still lower than the theoretically predicted values due to high recombination rates and low carrier mobilities.[24] Another direction in OPVs is to find economical electron acceptor alternatives to PCBM. One dimensional inorganic nanowires have been incorporated into the polymer blend[25–27] to create bulk heterojunctions. Nanowires are believed to enhance the exciton dissociation area and more importantly provide direct and efficient charge transport to the respective electrode. Morphological control *via* ordered microstructures has also been proposed where dimensions of both phases (acceptor and donor) can be controlled to minimize recombination and increase mobility *via* conjugated polymer chain stacking.[28] It has been demonstrated that hydrothermally grown ZnO NWs and P3HT can be utilized as electron acceptors and donors, respectively, for OPVs in the absence of PCBM.[29] In this paper, we combine these alternative approaches and describe the fabrication of flexible OPVs utilizing hydrothermally grown semi-aligned ZnO NW electron acceptors on top of solution deposited SWNT thin films.

Experimental

The OPV devices were fabricated as follows. First, SWNTs thin films were transferred on to polyethylene terephthalate (PET) substrates as described in detail elsewhere.[30] Briefly, HiPCO SWNTs purchased from CNI [Carbon Nanotechnologies Inc (batch R0496)] were thoroughly purified by several low temperature oxidative annealing and acid treatments and dispersed in

[a]*Department of Engineering, University of Cambridge, 9 JJ Thomson Avenue, Cambridge, UK CB0 0FA. E-mail: heu22@cam.ac.uk; Fax: +441223748322; Tel: +441223748318*
[b]*Department of Materials Science and Engineering, Rutgers University, 607 Taylor Road, Piscataway, New Jersey, 08854, USA. E-mail: manish1@rci.rutgers.edu; Fax: +17324453258; Tel: +1732445619*

This journal is © The Royal Society of Chemistry 2008

J. Mater. Chem., 2008, **18**, 5909–5912 | 5909

deionized water containing 1 wt% sodium dodecyl sulfate (SDS). The SWNTs were then vacuum filtered on mixed cellulose ester (MCE) membranes and transferred onto PET substrates. Solution concentration and filtration volume were 2 mg/L and 50 mL, respectively. Following deposition, SWNT thin films were functionalized by dipping in azeotropic nitric acid (69.7% HNO_3) for 3 hours and dried with a gentle nitrogen flow.[31] The scanning electron microscopy (SEM) image of a SWNT thin film uniformly coating the PET substrate surface is shown in Fig. 1a. Prior to functionalization, the sheet resistance of the SWNT thin film was 320 Ω/sq which decreased to 250 Ω/sq at a constant transparency of 65%. Following the functionalization step, formation of hydroxyl (OH) and carboxyl (COOH) groups was observed by IR absorption (not shown in here).

ZnO NWs were hydrothermally grown according to the method developed by Greene et al.[32] on functionalized SWNT thin films. Specifically, a 10 mM solution of zinc acetate dihydrate (98%, Aldrich) was prepared in 1-propanol (spectroscopic grade). The solution was then spin coated onto functionalized SWNT thin films at 2000 rpm for 30 s under ambient conditions. The substrates were then annealed at 100 °C for 1 min. Spin coating and annealing processes were repeated 10 times. After uniformly coating the SWNT thin films with ZnO seeds, vertical nanowires were grown by dipping the substrate in a mixture of equimolar 25 mM zinc nitrate hexahydrate ($Zn(NO_3)_2 \cdot 6H_2O$, Aldrich) and hexamethylenetetramine (HMTA) solution at 90 °C for 1 hour. Nitric acid treatment of the SWNT thin films was found to be crucial for uniform ZnO NW growth.
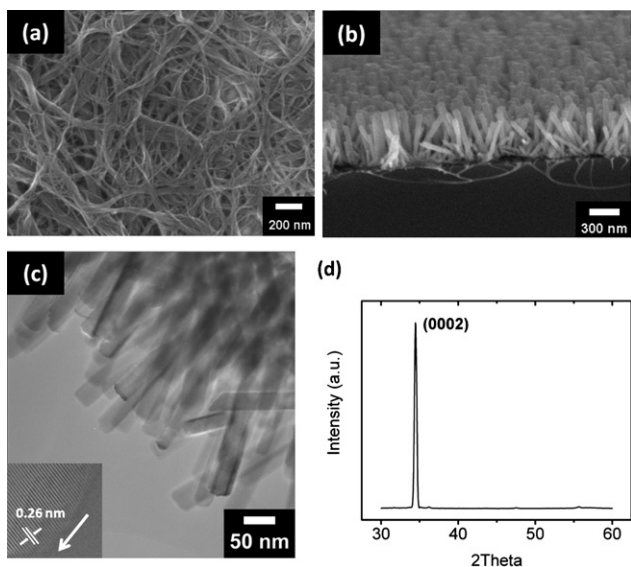

Fig. 1 The morphology and size of the SWNT thin films and ZnO nanowires were investigated by field emission scanning electron microscopy (FESEM) (JEOL 6340F, operated at 5kV). SEM image of (a) SWNT thin film on PET substrate with transparency and sheet resistance values of 65% and 320 Ω/sq, respectively. (b) ZnO nanowires grown hydrothermally on functionalized SWNT thin films. The single crystallinity of the ZnO nanowires was investigated by high resolution transmission electron microscopy (HRTEM) (JEOL 3011 operated at 300 kV). (c) TEM images of ZnO nanowires. The inset shows the HRTEM image of a single nanowire. The crystal structure of the ZnO nanowires was observed using X-ray diffraction (XRD) with a Philips PW1730 diffractometer with Cu Kα radiation. (d) XRD of nanowires.

We attribute this to better wetting of functionalized SWNT thin films by the seed particle solution. The substrates were then removed from the growth solution, rinsed with deionized water and annealed at 200 °C for 1 hour in argon atmosphere. The cross sectional SEM image of the SWNT/ZnO NW hybrid structures is shown in Fig. 1b. The diameters and lengths of the NWs on top of the SWNT thin films were found to range from 30–60 nm and 300–400 nm, respectively, after 1 hour growth time. Transmission electron microscopy (TEM) analysis of individual wires revealed that they are free of dislocations and stacking faults and indicated that they are oriented along the [0001] direction (Fig. 1c). This is consistent with the X-ray diffraction (XRD) results shown in Fig. 1d which also indicate that ZnO NWs preferentially grow along the [0001] direction. The roughness of the SWNT thin films ($\sim$25–50 nm) is most likely responsible for the slight misalignment of the nanowires indicated in the XRD spectrum.

Following the growth of ZnO NWs on top of SWNT thin films, regioregular P3HT (Rieke Metals) was spin coated (750 rpm) from a 25 mg/mL chloroform solution, followed by annealing at 120 °C for 10 minutes under argon atmosphere. Finally, a 100 nm thick Au top electrode was thermally evaporated in 10^{-6} mbar vacuum.

Results and discussions

The normal incidence transmittance of the SWNT thin films and ZnO NWs grown on SWNT thin films in the 1.5–4 eV photon energy range are shown in Fig. 2a. SWNT thin films show a relatively homogeneous transmission which provides sufficient light exposure in the P3HT to efficiently create excitons at the ZnO NW/P3HT interface. The highly crystalline ZnO nanowires also show good transmittance in the visible range. It should be noted that SWNT thin films are transparent in the UV range and therefore ZnO nanowires can absorb the incident UV light, contributing to charge carrier generation. The photovoltaic characteristics were evaluated using PET/SWNT/ZnO NW/P3HT/Au device configuration under AM 1.5 (100 mW/cm²) illumination and in dark. Samples were measured in air immediately after fabrication. External quantum efficiency (EQE) values were obtained using monochromatic light focused on the sample *via* a fiber optic cable and chopped at 20 Hz. A calibrated silicon photodiode was used to measure the light power. The current density versus voltage (J–V) curves for a device with the maximum observed conversion efficiency of $\sim$0.6% are shown in Fig. 2b. The device exhibited diode behavior in both dark and AM1.5 illumination The EQE results are shown in Fig. 2c where a maximum of 25% at 514 nm can be seen. Contributions to the photocurrent from both P3HT (400–700 nm) and ZnO (300–400 nm) are evident. The peak in the EQE spectrum at 370 nm results from absorption of ZnO and hole transfer to the P3HT.[29] The open circuit voltage of the devices was approximately 0.46V which is less than the bulk heterojunction energy offset ($\sim$0.7 V, see Fig. 3) but is comparable to the difference between the energy levels of the metallic SWNT Fermi level and the highest occupied molecular orbital of the P3HT. This suggests that the hole blocking layer formed from the seed layer at the SWNT and ZnO NW interface may not be completely uniform so that the bulk heterojunction between P3HT and the SWNTs may also occur.[33]
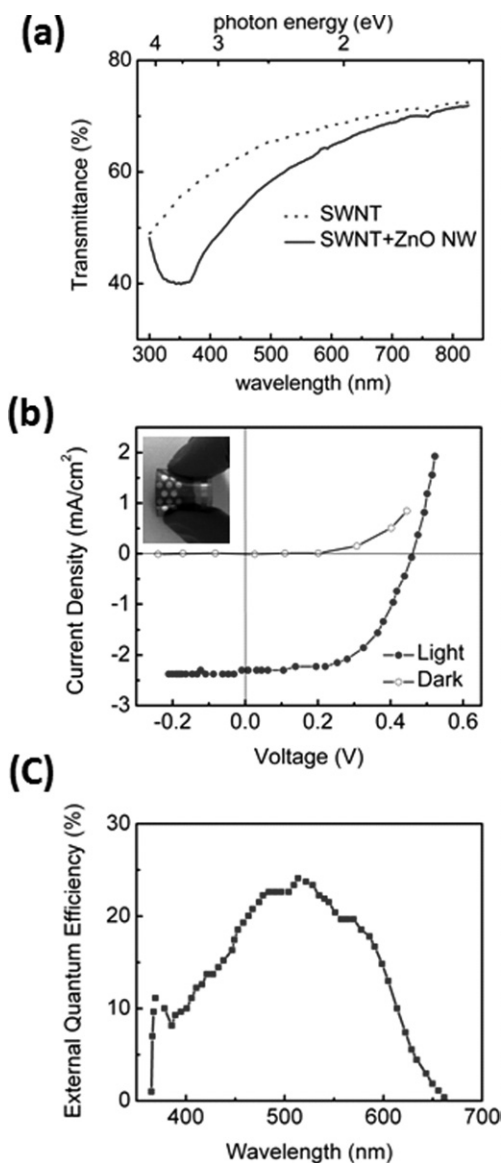
Fig. 2 (a) Optical transmittance versus wavelength of SWNT thin films and ZnO nanowires grown on SWNT thin films on PET substrate. The optical transparency was evaluated using a Thermoelectron Corporation UV/VIS Spectrometer UV2 in normal incidence mode. (b) Current density versus voltage curve for PET/SWNT/ZnO nanowire/P3HT/Au device at AM 1.5 light at 100 mW/cm² and in the dark. The inset shows an optical image of the PV device being flexed. The gold lines and spots are used for the contacts of the device. (c) EQE of the PET/SWNT/ZnO nanowire/P3HT/Au device.

Thus, the open circuit voltage and other OPV parameters may be the result of competing processes between the ZnO NW/P3HT and SWNT/P3HT bulk heterojunctions (see below).

In order to describe the origin of the photovoltaic effect, sufficiently efficient exciton dissociation and carrier transport must occur. The charge transfer and transport in the PET/SWNT/ZnO NW/P3HT/Au system can be understood with the aid of the energy diagram shown in Fig. 3. The band diagram schematically describes the exciton generation in P3HT, injection of electrons into the ZnO NWs and collection by the SWNT thin film electrode. The holes remain in the P3HT polymer and are
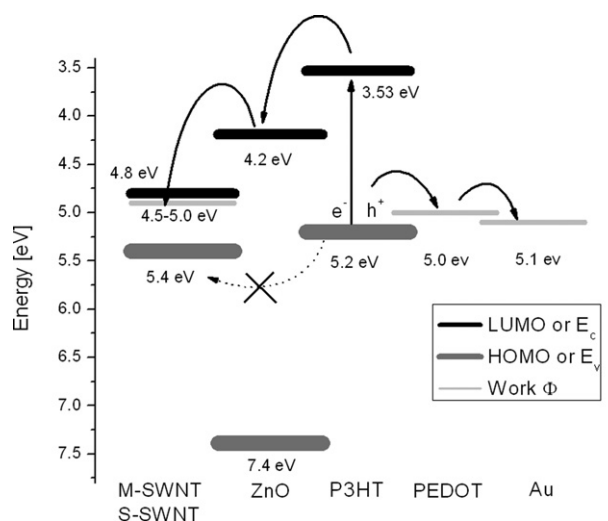

Fig. 3 Energy level diagram with respect to vacuum level for the PET/SWNT/ZnO nanowire/P3HT/Au device. The arrows indicate hole and electron flows. Ref. 35 was used to build this energy band diagram. M-SWNTs and S-SWNTs refer to metallic and semiconducting SWNTs, respectively.

collected by the gold top electrode. It should be noted that as-deposited and functionalized SWNT thin film networks are p-type. However, since the SWNT thin films used in the OPV devices are deposited using a concentration and filtration volume that is substantially above the percolation threshold for metallic SWNTs, electron collection is mostly facilitated by the metallic SWNTs.

Examination of the energy levels at the ZnO/P3HT interface readily reveals that the barrier for hole injection from the P3HT is very large, whereas there is no barrier for electron injection. Hence there is preferred collection of electrons by the ZnO NWs. Closer observation of the SWNT thin film and ZnO NW hybrid interface reveals the presence of a semi-continuous ZnO thin film formed from the zinc acetate precursor (or the seed layer) which electrically isolates the bulk heterojunctions from the SWNT thin film.[34] The presence of this interface layer is important as it prevents hole injection into the SWNTs because the energetics for hole transfer from the ZnO NWs into the SWNT thin films are not favorable. Thus, it is more likely that the electrons are injected into the ZnO NWs and collected by the metallic SWNTs. In addition, the semi-continuous ZnO thin film at the interface prevents injection of holes directly into the SWNTs via the bulk heterojunction effect between the P3HT and SWNTs.[33]

The maximum efficiency values we obtained from these devices were ~0.6% which is much lower than the state-of-the-art P3HT/PCBM devices. There are several reasons for this including the competition between any residual SWNT/P3HT and ZnO NW/P3HT bulk heterojunctions. This limits the open circuit voltage to that of residual SWNT/P3HT junction path which acts in parallel to that of the ZnO NW/P3HT junction. That is, in the P3HT/SWNT bulk heterojunctions, holes are injected into the SWNT electrodes which would recombine with the electrons collected from the ZnO NW/P3HT bulk heterojunctions, limiting the overall efficiency of the devices. Another reason is the fact that the volume of P3HT within the voids between the ZnO nanowires is significantly diminished, reducing the concentration

This journal is © The Royal Society of Chemistry 2008

J. Mater. Chem., 2008, **18**, 5909–5912 | 5911

of photogenerated carriers. It has also been suggested that for P3HT/ZnO NW OPVs on ITO, excitons may not dissociate at the P3HT/ZnO interface at all and that the free carriers are generated directly in P3HT. This model is controversial, however, and our present study does not provide any specific insight to suggest that the free carriers are produced in P3HT alone and not at the P3HT/ZnO interface.

Our device utilizes an inverted geometry so that the reactive aluminium electrode is avoided.[36] This would in turn increase the operational stability of the device under atmospheric conditions. In addition, stability of hybrid polymer/metal oxide systems has already been reported for several metal oxides.[37–39] In the case of ZnO, it has been shown that oxygen vacancies in ZnO could be quenched upon air/oxygen exposure which reduces the carrier concentration and improves the device performance as compared to devices stored in a protective atmosphere.[39] SWNTs are inherent sources of oxygen due to physisorption on the side walls. Carboxylic acid functionalized SWNTs, in our case, contain a high oxygen content due to chemisorption. SWNT thin films would continuously supply oxygen to the ZnO nanowires lying on top. This transfer of oxygen to ZnO nanowires would be more efficient compared to the supply of oxygen from the environment. Thus, the preparation conditions (protective atmosphere/air) had no clear effect on the performance of the device. We thus tentatively attribute the relatively high performance in our device, as compared to other works on P3HT/ZnO nanowires, to the continuous supply of oxygen from the SWNT thin films. Detailed analysis on the oxygen content and device lifetime measurements for our system are currently in progress.

Conclusions

In summary, we have demonstrated that ZnO nanowires can be grown hydrothermally on SWNT thin films. The results suggest that these SWNT/ZnO NW hybrid nanostructures could be useful for flexible OPVs to serve as electron collecting electrodes combined with an electron acceptor. In addition, the use of ZnO NWs instead of functionalized fullerenes (i.e. PCBM) provides a cost effective alternative for OPVs. The observed enhancement of the response in the blue–near UV region through absorption by the ZnO NWs is beneficial for OPV cells/surfaces designed for harvesting background energy from indoor artificial light sources. Finally, the nanotube–nanowire hybrid structures maybe promising for applications in nanoscale systems, including new electronic and photonic devices.

Acknowledgements

References

1 S. S. Sun, N. S. Sariciftci (Eds.) *Organic Photovoltaics: Mechanism, Materials and Devices*, Taylor & Francis, London, 2005.

2 C. J. Brabec, V. Dyakonov, J. Parisi, N. S. Sariciftci (Eds.), *Organic Photovoltaics: Concepts and Realization*, Springer Verlag, Heidelberg, 2003.

3 H. Spanggaard and F. C. Krebs, *Sol. Energy Mater. Sol. Cells*, 2004, **83**, 125.

4 K. M. Coakley and M. D. McGehee, *Chem. Mater*, 2004, **16**, 4533.

5 H. Hoppe and N. S. Sariciftci, *J. Mater. Res.*, 2004, **19**, 1924.

6 S. Gunes, H. Neugebauer and N. S. Sariciftci, *Chem. Rev.*, 2007, **107**, 1324.

7 B. C. Thompson and J. M. J. Frechet, *Angew. Chem. Intl. Ed.*, 2008, **47**, 58.

8 G. Li, V. Shrotriya, J. Huang, Y. Yao, T. Moriarty, K. Emery and Y. Yang, *Nat. Materials*, 2005, **4**, 864.

9 M. Reyes-Reyes, K. Kim and D. L. Carroll, *Appl. Phys. Lett.*, 2005, **87**, 083506.

10 C. Winder and N. S. Sariciftci, *J. Mater. Chem.*, 2004, **14**, 1077.

11 E. Bundgaard and F. C. Krebs, *Sol. Energy Mater. Sol. Cells*, 2007, **91**, 954.

12 G. Li, V. Shrotriya, J. S. Huang, Y. Yao, T. Moriarty, K. Emery and Y. Yang, *Nat. Mater.*, 2005, **4**, 864.

13 S. Miller, G. Fanchini, Y.-Y. Lin, C. Li, C.-W. Chen, W.-F. Su and Manish Chhowalla, *J. Mater. Chem.*, 2008, **18**, 306.

14 M. Jorgensen, K. Norrman and F. C. Krebs, *Sol. Energy Mater. Sol. Cells*, 2008, **92**, 686.

15 J. A. Hauch, P. Schilinsky, S. A. Choulis, S. Rajoelson and C. J. Brabec, *Appl. Phys. Lett.*, 2008, **93**, 103306.

16 T. Aernouts, P. Vanlaeke, W. Geens, J. Poortmans, P. Heremans, S. Borghs, R. Mertens, R. Andriessen and L. Leenders, *Thin Solid Films*, 2004, **451**, 22.

17 B. Winther-Jensen and F. C. Krebs, *Sol. Energy Mater. Sol. Cells*, 2006, **90**, 123.

18 J.-Y. Lee, S. T. Connor, Y. Cui and P. Peumans, *Nano Lett.*, 2008, **8**, 689.

19 E. Kymakis, I. Alexandrou and G. A. J. Amaratunga, *J. Appl. Phys.*, 2003, **93**, 1764.

20 H. Ago, K. Petritsch, M. S. P. Shaffer, A. H. Windle and R. H. Friend, *Adv. Mater.*, 1999, **11**, 1281.

21 A. J. Miller, R. A. Hatton and P. S. Ravi Silva, *Appl. Phys. Lett.*, 2006, **89**, 133117.

22 A. Du Pasquier, H. E. Unalan, A. Kanwal, S. Miller and M. Chhowalla, *Appl. Phys. Lett.*, 2005, **87**, 203511.

23 M. W. Rowell, M. A. Topinka, M. D. McGehee, H.-J. Prall, G. Dennler, N. S. Sariciftci, L. Hu and G. Gruner, *Appl. Phys. Lett*, 2006, **88**, 233506.

24 L. J. A. Koster, V. D. Mihailetchi and P. W. M. Blom, *Appl. Phys. Lett.*, 2006, **88**, 093511.

25 W. U. Huynh, J. J. Dittmer and A. P. Alivisatos, *Science*, 2002, **295**, 2425.

26 W. U. Huynh, J. J. Dittmer, W. C. Libby, G. L. Whiting and A. P. Alivisatos, *Adv. Funct. Mater.*, 2003, **13**, 73.

27 C. H. Chang, T. K. Huang, Y. T. Lin, Y. Y. Lin, C. W. Chen, T. H. Chu and W. F. Su, *J. Mater. Chem.*, 2008, **18**, 2201.

28 K. M. Coakley, Y. Liu, C. Goh and M. D. McGehee, *MRS Bulletin*, 2005, **30**, 37.

29 D. C. Olson, J. Piris, R. T. Collins, S. E. Shaheen and D. S. Ginley, *Thin Solid Films*, 2006, **496**, 26.

30 H. E. Unalan, G. Fanchini, A. Kanwal, A. Du Pasquier and M. Chhowalla, *Nano. Lett.*, 2006, **6**, 677.

31 B. B. Parekh, G. Fanchini, G. Eda and M. Chhowalla, *Appl. Phys. Lett.*, 2007, **90**, 121913.

32 L. E. Greene, M. Law, D. H. Tan, M. Montano, J. Goldberger, G. Somorjai and P. Yang, *Nano. Lett.*, 2005, **5**, 1231.

33 Y. Y. Lin, S. Miller, B. Parekh, G. Eda, G. Fanchini, C. W. Chen, W. F. Su and M. Chhowalla, unpublished results.

34 A. M. Peiro, P. Ravirajan, K. Govender, D. S. Boyle, P. O'Brien, D. D. C. Bradley, J. Nelson and J. R. Durrant, *J. Mater. Chem.*, 2006, **16**, 2088.

35 R. Ravirajan, A. M. Peiro, M. K. Nazeeruddin, M. Graetzel, D. D. C. Bradley, J. R. Durrant and J. Nelson, *J. Phys. Chem. B*, 2006, **110**, 7635.

36 M. S. White, D. C. Olson, S. E. Shaheen, N. Kopidakis and D. S. Ginley, *Appl. Phys. Lett.*, 2006, **89**, 143517.

37 M. Lira-Cantu and F. C. Krebs, *Sol. Energy Mater. Sol. Cells*, 2006, **90**, 2076.

38 F. C. Krebs, *Sol. Energy Mater. Sol. Cells*, 2008, **92**, 715.

39 D. C. Olson, S. E. Shaheen, R. T. Collins and D. S. Ginley, *J. Phys. Chem. C*, 2007, **111**, 16670.